

# Recipes for improper ferroelectricity in hybrid perovskites

Hanna L. B. Boström<sup>1</sup>, Mark S. Senn<sup>1,2</sup> & Andrew L. Goodwin<sup>1</sup>

<sup>1</sup>*Department of Chemistry, University of Oxford, South Parks Road, OX1 3QR, Oxford, UK*

<sup>2</sup>*Department of Chemistry, University of Warwick, Gibbet Hill, CV4 7AL, Coventry, UK*

**The central goal of crystal engineering is to develop precise control over material function *via* rational design of structure. A particularly successful realisation of this paradigm is the example of hybrid improper ferroelectricity in layered perovskite materials, where cation vacancies and cooperative octahedral tilts combine to break inversion symmetry. However, in the more chemically diverse and technologically relevant family of inorganic ABX<sub>3</sub> perovskites, symmetry conspires to render hybrid coupling to polar distortions impossible. In this study, we use group-theoretical analysis to uncover a profound enhancement of the number of improper ferroelectric coupling schemes available to *molecular* perovskites. This enhancement arises because molecular substitution on the A- and/or X-site significantly diversifies the range of distortions possible. Not only do our insights rationalise the emergence of polarisation in a number of previously-studied materials, but we identify the fundamental importance of molecular degrees of freedom at the A-site, which are much more straightforwardly controlled from a synthetic viewpoint than are lattice, charge and orbital degrees of freedom. We envisage that the crystal design principles we develop here will be enable targeted synthesis of a large family of new acentric functional materials.**

Ferroelectricity, *i.e.* the presence of a switchable electric polarisation, is an important property with many technological applications.<sup>1</sup> An early canonical ferroelectric was BaTiO<sub>3</sub>, with the broader family of ABX<sub>3</sub> perovskite oxides now known to include a variety of ferroelectric systems.<sup>2-5</sup> The ferroelectric response of BaTiO<sub>3</sub> originates from a second-order Jahn-Teller (SOJT) effect, in which the B-site cation Ti displaces from the centre of its TiO<sub>6</sub> coordination environment.<sup>2,6</sup> As this polar instability also acts as the primary order parameter, BaTiO<sub>3</sub> is a proper ferroelectric. Despite the continuing discussion regarding the origin of polar coupling in BaTiO<sub>3</sub>,<sup>7</sup>

the general SOJT mechanism at play is rare and difficult to generalise because it requires a  $d^0$  electronic configuration.<sup>6</sup> Hence design approaches for new ferroelectric materials based on SOJT instabilities are limited and, what's more, the mechanism is inherently incompatible with spin-active  $d$ -electron configurations, which has largely prevented its exploitation in the search for magneto-electric multiferroics.<sup>8</sup> In fact, ferroelectricity is comparatively rare in bulk perovskite materials and  $\text{BaTiO}_3$  is much more of an exception than a rule.<sup>9</sup>

It is in this context that the concept of hybrid improper ferroelectricity is especially appealing.<sup>10</sup> A necessary condition for ferroelectricity is the presence of a polar space group, which in turn requires broken inversion symmetry. Simple inorganic perovskites contain two crystallographically distinct inversion centres (at the A- and B-site, respectively) and in  $\text{BaTiO}_3$ , the zone-centre polar mode breaks both of these, driving the polarity.<sup>11</sup> Alternatively, in favourable cases, a combination of two or more modes—each non-polar in their own right—may collectively lift inversion symmetry and give rise to a polar secondary order parameter.<sup>10,12</sup> This so-called hybrid improper ferroelectricity mechanism is attractive from a crystal engineering perspective because it lends itself to design rules *via* group-theoretical analysis.<sup>10</sup> In addition, the mechanism does not preclude magnetic order.<sup>10,13</sup> So, using group-theoretical methods, it is possible to enumerate the symmetry breaking caused by given distortions of an aristotype and thereby predict the propensity for the formation of acentric structures. For simple inorganic perovskites, the accessible degrees of freedom—cooperative first-order Jahn-Teller (FOJT) distortions and octahedral tilting—all preserve the inversion centre of the B-site, and in order to enable hybrid improper ferroelectricity, additional symmetry breaking in the form of A-site cation order or layering is needed.<sup>13–15</sup>

A recent development in the broader field is the increased interest in molecular perovskite analogues.<sup>16</sup> These are solid compounds with the same  $\text{ABX}_3$  stoichiometry of conventional perovskites, but where A or X (or both) are molecular ions. This populous class of materials may be categorised according to the nature of the anionic linker: topical families include the organic-halide perovskites,<sup>17,18</sup> metal formates,<sup>19,20</sup> Prussian blue analogues,<sup>21,22</sup> azides,<sup>23,24</sup> dicyanamides,<sup>25,26</sup> thiocyanates,<sup>27,28</sup> and dicyanometallates.<sup>29,30</sup> The enhanced structural flexibility allowed by molec-

ular species enables additional degrees of freedom unfeasible in conventional inorganic perovskites: unconventional tilts,<sup>29,31</sup> columnar shifts,<sup>32</sup> and multipolar order [Fig. 1].<sup>33,34</sup> The first two of these correspond to rigid-unit modes<sup>35</sup>—*i.e.* phonon modes which propagate without deforming  $\text{BX}_6$  coordination geometries<sup>36,37</sup>—whereas the third degree of freedom concerns reorientations of molecular A-site cations.<sup>33,34,38</sup> In this paper, we show how these new types of structural degrees of freedom can combine to remove centrosymmetry, hence establishing a new set of design rules for engineering acentric molecular perovskites. Our study is arranged as follows. First, we introduce our general recipe for designing acentric materials. Second, we classify the various symmetry-breaking ingredients accessible to molecular perovskites in terms of the irreducible representations of the high symmetry perovskite aristotype. Third, we use these ingredients to construct the key ferroelectric coupling schemes. And, fourth, we illustrate how this approach can be used to rationalise the emergence of polarisation in a number of previously-reported systems.

## Results

The fundamental idea of our approach is to identify two distortions ( $A$  and  $B$ ) of the parent  $Pm\bar{3}m$  aristotype that are inherently non-polar but which, when combined, give rise to an additional polar degree of freedom ( $P$ ) in the “child” distorted structure. In a Landau-style expansion of the free energy about the parent structure, this produces a third-order (trilinear) term  $\beta ABP$ . As  $A$  and  $B$  are inherently non-zero if they are unstable with respect to the parent phase then—irrespective of the sign of the coefficient  $\beta$ — $P$  will also adopt a non-zero (positive or negative) value in order to stabilise the free energy. We can use the idea of invariants analysis<sup>39</sup> to identify the permissible third-order terms in the general free energy expansion; *i.e.* identify for which combinations of  $A$  and  $B$  one would expect coupling to  $P$ . For the zone-boundary/zone-centre distortions that we consider here, we find that such couplings may in fact be identified by inspection, as detailed in the following paragraphs.

Each distortion we consider can be described as transforming as an irreducible representation (irrep) of the parent space group  $Pm\bar{3}m$  [Table 1, see Fig. S1 and Table S1 for a more compre-

hensive list]. The irrep labels are of the form  $\mathbf{k}_{\#}^{+/-}$ , where the letter  $\mathbf{k}$  denotes the propagation or wave vector of the distortion with respect to the parent structure. In our study we consider  $\mathbf{k} = [0, 0, 0]$  ( $\Gamma$ ),  $[\frac{1}{2}, \frac{1}{2}, \frac{1}{2}]$  ( $R$ ),  $[\frac{1}{2}, \frac{1}{2}, 0]$  ( $M$ ),  $[0, \frac{1}{2}, 0]$  ( $X$ ), and symmetry equivalents thereof—these being the distortion periodicities most relevant to real examples. The + or – sign generally denotes that either one or the other inversion centre, related to each other by a origin shift (*i.e.* a translation by  $\frac{1}{2}, \frac{1}{2}, \frac{1}{2}$ ), is broken. Clearly, any collective ordering or distortion that fails to break both these inversion centres at once cannot lead to an improper ferroelectric coupling, and it is this point that underlies our arguments based on invariants analysis presented below.

As any term that features in the free energy expansion about the parent phase must conserve both crystal momentum and parity with respect to inversion symmetry, it can quickly be seen that any two distortions transforming as  $X^+$  and  $X^-$ , or as  $M^+$  and  $M^-$ , or as  $R^+$  and  $R^-$  must couple to a non-centrosymmetric (and in general polar) distortion  $P$ , which itself transforms as  $\Gamma^-$ . On the other hand, any two distortions to the parent phase that have either a different propagation vector and/or the same sign with respect to inversion parity, cannot produce such a coupling to  $P$ . Hence, couplings such as  $X^+$  and  $R^-$ , or  $M^-$  and  $M^-$  *etc.*, may be immediately discounted. As a final point, we note that higher-order coupling terms such as  $(X^+, M^+, R^-)$ ,  $(X^-, M^-, R^-)$  and so on also produce a fourth order coupling in  $P$ , provided that the rules for preservation of crystal-momentum and parity are observed.

In the context of molecular perovskites, the relevant collective distortions involve (i) conventional tilts, (ii) unconventional tilts, (iii) columnar shifts, (iv) FOJT effects, and (v) multipolar A-site order. The combinations of distortions capable of driving polarity are shown in Fig. 2, with an example of a representative child space group given for each specific combination. For analysis of related third- and fourth-order coupling schemes, see Table S2 and S3. Our main result is the clear distinction in number of possibilities for inversion symmetry breaking in molecular perovskites relative to their inorganic counterparts [inset in Fig. 2]. Indeed we find that either multipolar order (driven by molecular substitution on the A-site) or the activation of columnar shifts (driven by molecular substitution on the X-site) is by itself sufficient to break inversion symmetry

when correctly coupled to any other order parameter. Hence in the design of ferroelectric molecular perovskites, molecular substitution need involve only one site (A or X) and polar ground states are theoretically possible both for A-site-only substituted perovskites (*e.g.* the organic–halide perovskites) and for their X-site-only substituted cousins (*e.g.* Prussian blue analogues).

Arguably the easiest distortion to control from a materials design perspective is that of A-site multipolar order. Many common organic cations are polar—their charge being localised on a single atom. Moreover both rod-like (prolate) and disc-like (oblate) cations possess quadrupole moments. This includes common cations such as methylammonium ( $\text{CH}_3\text{NH}_3^+$ ), hydrazinium ( $\text{NH}_2\text{NH}_3^+$ ), guanidinium ( $\text{C}(\text{NH}_2)_3^+$ ) and imidazolium. Higher-order multipoles are also possible, such as the hexapole moment of guanidinium and the octupole moment of ammonium and tetramethylammonium. Table 1 makes clear that equivalent types of zone-boundary dipolar and quadrupolar order transform as irreps with opposite sign with respect to inversion parity. Hence the incorporation of cations which support both dipole and quadrupole moments gives access to a greatly increased number of possible improper couplings to bulk polarisation.

For inorganic perovskites the most common space group is  $Pnma$ :<sup>40</sup> this crystal symmetry arises from a combination of in-phase  $M_2^+$  and out-of-phase  $R_5^-$  tilting mode. An additional antiferroelectric A-site cation displacement transforming as  $X_5^-$  appears as a secondary order parameter. Based on the results presented above, it is relevant to ask what distortions need to be added to this very common structure to generate bulk polarisation? Recalling the requirement to combine separate distortions together transforming as irreps with the same propagation vector but opposite sign with respect to inversion parity, it is clear that quadrupolar A-site order transforming as  $R_5^+$  or  $X_5^+$  irreps may provide the required coupling with the octahedral rotations ( $R_5^-$ ) or anti-polar distortions ( $X_5^-$ ) present in the  $Pnma$  structure. Alternatively, dipolar ordering transforming as  $M_3^-$  or  $M_5^-$  could couple to the octahedral rotations at the M-point ( $M_2^+$ ), and clearly any dipolar ordering at the  $\Gamma$ -point necessitates an overall polar structure. Hence, a molecular cation with both a dipolar moment and quadrupole moment, enclosed in a  $Pnma$  perovskite, will give rise to hybrid improper ferroelectricity, provided that the dipole moment orders at the  $\Gamma$ - or M-point or the

quadrupole moment orders at the X- or R-point. To maximise the likelihood of such a situation, it is advisable to choose cations with both quadrupolar and dipolar moments, of which there are plenty of examples, *e.g.* hydrazinium, imidazolium, and methylammonium. Steric considerations will stabilise orientational order of larger cations to lower temperatures, and design rules for controlling the type of quadrupolar order are now starting to emerge.<sup>34</sup> Hence, judicious choice of a molecular cation with the correct type of multipole moment may thus be an important design strategy for engineering hybrid improper ferroelectricity.

There are a number of hybrid ferroelectric molecular perovskites already reported in the literature and we proceed to rationalise the emergence of polarisation in these systems in light of the analysis presented above. For ease of illustration, we give two-dimensional representations of the relevant coupling schemes in Fig. 3. Our first example is that of the formate perovskite  $\text{NH}_4\text{Cd}(\text{HCOO})_3$ , first synthesised several decades ago<sup>41</sup> and revisited more recently for its dielectric properties.<sup>42</sup> The system crystallises in the polar space group  $Pna2_1$ , with the formate anion adopting a mixed *syn-anti* binding mode. This binding geometry is less prevalent than the *anti-anti* binding mode typically observed for formate-bridged perovskites,<sup>20,43–46</sup> and is related to the low tolerance factor.<sup>46</sup> The structure contains a considerable planar shift alternating along the *c* direction which is described by the irrep  $X_5^+$ . It also supports an unconventional tilt, which transforms as  $X_5^-$ . These distortions yield the polar space group  $Cmc2_1$ , which in combination with the conventional in-phase tilting ( $M_2^+$ ) gives  $Pna2_1$ . Despite the fact that three order parameters are needed to fully account for the observed space group, the shift ( $X_5^+$ ) and unconventional tilt ( $X_5^-$ ) are sufficient to account for inversion-symmetry breaking.

Our second example is that of  $\text{GuaCu}(\text{HCOO})_3$  (where  $\text{Gua} = \text{C}(\text{NH}_2)_3^+$ ), which also crystallises in  $Pna2_1$ . In this case the coupling is between a cooperative Jahn–Teller distortion and multipolar A-site order. It is the only polar member of the family  $\text{GuaM}(\text{HCOO})_3$  ( $M = \text{Mn}, \text{Fe}, \text{Co}, \text{Ni}, \text{Cu}, \text{Zn}, \text{Cd}$ ),<sup>43,47</sup> and also the only Jahn–Teller-active member of the same family, which immediately identifies the importance of a collective Jahn–Teller distortion ( $M_3^+$ ) in the coupling scheme. The multipolar order associated with the particular alignment of the Gua couches in fact

two order parameters: the quadrupolar ordering  $X_5^+$  (orientation of the G<sub>ua</sub> plane normal) and the hexapolar ordering (specific orientation around the three-fold axis). The role of collective JT order in driving inversion-symmetry breaking in this system has been identified previously, as has the intriguing possibility of magnetoelectric coupling in this same system.<sup>48,49</sup>

So we can conclude that, from a group-theoretical viewpoint, perovskites with a molecular component are remarkably predisposed to crystallising in polar space groups. This attractive property is a result of the large number of polar coupling schemes generated by distortions accessible to molecular perovskites but inaccessible to conventional inorganic perovskites. We have identified specific combinations of structural distortions that lead to acentric structures and have thereby suggested possible routes for targeted material design. In addition, we have found that either A-site quadrupolar order or the activation of columnar shifts—features that are unique to molecular perovskites—can drive polarisation when coupled to conventional (*Pnma*-type) distortions of the perovskite structure. There are several examples of hybrid improper ferroelectric coupling—although not always recognised as such—already present in the literature and we fully anticipate further examples will continue to emerge. Despite the fact that our analysis has been focused on polarisation in formate perovskite analogues, the general rules developed here extend to *all* molecular perovskites and to *all* applications where inversion symmetry breaking is necessary. A recent example is the development of non-linear optics based on dicyanamide perovskite chemistry.<sup>50</sup>

## Methods

A hypothetical aristotype molecular perovskite was employed as our model system, with the space group  $Pm\bar{3}m$  and the (monoatomic) A-site cation at  $1a$  (0, 0, 0), B-site cation at  $2a$  ( $\frac{1}{2}$ ,  $\frac{1}{2}$ ,  $\frac{1}{2}$ ) and X-site anion at  $6f$  ( $\frac{1}{2}$ ,  $\frac{1}{2}$ ,  $z$ ). The formula is thus  $AB(X_2)_3$ . This was used as an input to the web-based software ISODISTORT,<sup>51</sup> and the rigid-unit modes and orbital ordering patterns could be identified by inspection.

Multipoles may be classified as transforming as irreps of the rotational group  $SO(3)$ . In the absence of any external perturbations to the rotational symmetry (*i.e.* a completely spherically symmetric crystal field), monopoles (angular component of  $s$  orbital) transform as a singly degenerate irrep, dipoles ( $p$ ) as triply degenerate, quadrupoles ( $d$ ) as 5-fold degenerate, *etc.* To determine the effect on the irreps of lowering the symmetry of  $SO(3)$ , such as occurs at any site symmetry in any crystallographic group, we can use descent of symmetry tables. For quadrupoles, if one or more of the irreps enters the symmetric representation ( $A_{1g}$ ), then we may consider the action of lowering the point group symmetry to have resulted in multipolar order [and this is how we define quadrupolar order in the context of this paper]. In the aristotype  $ABX_3 Pm\bar{3}m$  structure quadrupoles (*i.e.*  $d$ -orbitals) centred at A/B transform as  $E_g$  and  $T_{1g}$  while at X they transform as  $A_{1g}$ ,  $B_{1g}$ ,  $B_{2g}$ ,  $E_g$ . Hence, the problem of determining whether a given irrep of space group  $Pm\bar{3}m$  implies quadrupolar order is reduced to determining whether its action as a primary order parameter is sufficient to lower the point-group symmetry at A/B/X such that an additional quadrupole (degree of freedom) enters the totally symmetric representation.

In order to ensure that all relevant irreps for quadrupolar (or multipolar) orders were considered, a dummy atom was placed on  $48n (x, y, z)$  in order to mimic electron density in the unit cell at the most general position. We use a setting where the A-site is located at the origin of the perovskite unit cell [See Table S1 for conversion to the other setting]. For each relevant point of the Brillouin zone, we test in turn the action of an order parameter transforming as one of these irreps, and list its effect on lowering the point group symmetry at A, B and X, and hence the degree of quadrupolar order they correspond to. We start by considering the  $\Gamma$ -point irreps, a process which corresponds to ascertaining the relationship between lattice strain and multipolar order. Next we consider high-symmetry order parameter directions (OPDs) for the zone-boundary irreps which, where possible, we choose such that there are no secondary order parameters. This is important, since many primary order parameters transforming as zone-boundary irreps will imply a lattice strain and hence indirectly induce quadrupolar order at the  $\Gamma$ -point, but do not themselves correspond to such a ordering at the X/M/R-points. Where it is not possible to find a high-symmetry OPD with associated isotropy subgroup without secondary order parameters (SOPs), a process of



elimination is used, subtracting the degree of quadrupolar ordering implied by each SOPs in turn. In such a manner it was possible to identify unambiguously which irreps were associated with quadrupolar order.

1. Scott, J. F. Applications of modern ferroelectrics. *Science* **315**, 954–959 (2007).
2. von Hippel, A., Breckenridge, R. G., Chesley, F. G. & Tisza, L. High dielectric constant ceramics. *Ind. Eng. Chem.* **38**, 1097–1109 (1946).
3. Matthias, B. T. Ferroelectricity. *Science* **113**, 591–596 (1951).
4. Cohen, R. E. Origin of ferroelectricity in perovskite oxides. *Nature* **358**, 136–138 (1992).
5. Randall, C. A., Bhalla, A. S., Shrout, T. R. & Cross, L. E. Classification and consequences of complex lead perovskite ferroelectrics with regard to B-site cation order. *J. Mater. Res.* **5**, 829–834 (1990).
6. Burdett, J. K. Use of the Jahn-Teller theorem in inorganic chemistry. *Inorg. Chem.* **20**, 1959–1962 (1981).
7. Senn, M. S., Keen, D. A., Lucas, T. C. A., Hriljac, J. A. & Goodwin, A. L. Emergence of long-range order in BaTiO<sub>3</sub> from local symmetry-breaking distortions. *Phys. Rev. Lett.* **116**, 207602 (2016).
8. Spaldin, N. A. Why are there so few magnetic ferroelectrics? *J. Phys. Chem. B* **104**, 6694–6709 (2000).
9. Benedek, N. A. & Fennie, C. J. Why are there so few perovskite ferroelectrics? *J. Phys. Chem. C* **117**, 13339–13349 (2013).
10. Benedek, N. A. & Fennie, C. J. Hybrid improper ferroelectricity: A mechanism for controllable polarization-magnetization coupling. *Phys. Rev. Lett.* **106**, 107204 (2011).
11. Hewat, A. W. Structure of rhombohedral ferroelectric barium titanate. *Ferroelectrics* **6**, 215–218 (1974).

12. Benedek, N. A., Rondinelli, J. M., Djani, H., Ghosez, P. & Lightfoot, P. Understanding ferroelectricity in layered perovskites: new ideas and insights from theory and experiments. *Dalton Trans.* **44**, 10543–10558 (2015).
13. Pitcher, M. J. *et al.* Tilt engineering of spontaneous polarization and magnetization above 300 K in a bulk layered perovskite. *Science* **347**, 420–424 (2015).
14. Rondinelli, J. M. & Fennie, C. J. Octahedral rotation-induced ferroelectricity in cation ordered perovskites. *Adv. Mater.* **24**, 1961–1968 (2012).
15. Oh, Y. S., Luo, X., Huang, F.-T., Wang, Y. & Cheong, S.-W. Experimental demonstration of hybrid improper ferroelectricity and the presence of abundant charged walls in  $(\text{Ca,Sr})_3\text{Ti}_2\text{O}_7$  crystals. *Nat. Mater.* **14**, 407–413 (2015).
16. Li, W. *et al.* Chemically diverse and multifunctional hybrid organic-inorganic perovskites. *Nat. Rev. Mater.* **2**, 16099 (2017).
17. Weber, D.  $\text{CH}_3\text{NH}_3\text{SnBr}_x\text{I}_{3-x}$  ( $x = 0 - 3$ ) - Sn(II)-system with cubic perovskite structure. *Z. Naturforsch. B* **33**, 862–865 (1978).
18. Saparov, B. & Mitzi, D. B. Organic-inorganic perovskites: Structural versatility for functional materials design. *Chem. Rev.* **116**, 4558–4596 (2016).
19. Sletten, E. & Jensen, L. H. The crystal structure of dimethylammonium copper(II) formate,  $\text{NH}_2(\text{CH}_3)_2[\text{Cu}(\text{OOCH})_3]$ . *Acta Cryst. B* **29**, 1752–1756 (1973).
20. Jain, P., Dalal, N. S., Toby, B. H., Kroto, H. W. & Cheetham, A. K. Order-disorder antiferroelectric phase transition in a hybrid inorganic-organic framework with the perovskite architecture. *J. Am. Chem. Soc.* **130**, 10450–10451 (2008).
21. Xu, W.-J. *et al.* Cation-dependent structural phase transition and dielectric response in a family of cyano-bridged perovskite-like coordination polymers. *Dalton Trans.* **45**, 4242–4229 (2016).
22. Buser, H. J., Schwarzenbach, D., Petter, W. & Ludi, A. The crystal structure of Prussian Blue:  $\text{Fe}_4[\text{Fe}(\text{CN})_6]_3 \cdot x\text{H}_2\text{O}$ . *Inorg. Chem.* **16**, 2704–2710 (1977).

23. Zhao, X.-H. *et al.* Cation-dependent magnetic ordering and room-temperature bistability in azido-bridged perovskite-type compounds. *J. Am. Chem. Soc.* **135**, 16006–16009 (2013).
24. Du, Z.-Y. *et al.* Structural transition in the perovskite-like bimetallic azido coordination polymers  $(\text{NMe}_4)_2[\text{B}'\cdot\text{B}''(\text{N}_3)_6]$  ( $\text{B}' = \text{Cr}^{3+}, \text{Fe}^{3+}$ ;  $\text{B}'' = \text{Na}^+, \text{K}^+$ ). *Cryst. Growth Des.* **14**, 3903–3909 (2014).
25. Schlueter, J. A., Manson, J. L., Hyzer, K. A. & Geiser, U. Spin canting in the 3D anionic dicyanamide structure  $(\text{SPh}_3)\text{Mn}(\text{dca})_3$  ( $\text{Ph} = \text{phenyl}$ ,  $\text{dca} = \text{dicyanamide}$ ). *Inorg. Chem.* **43**, 4100–4102 (2004).
26. Tong, M.-L. *et al.* Cation-templated construction of three-dimensional  $\alpha$ -Po cubic-type  $[\text{M}(\text{dca})_3]$  networks. Syntheses, structures and magnetic properties of  $\text{A}[\text{M}(\text{dca})_3]$  ( $\text{dca} = \text{dicyanamide}$ ; for  $\text{A} = \text{benzyltributylammonium}$ ,  $\text{M} = \text{Mn}^{2+}, \text{Co}^{2+}$ ; for  $\text{A} = \text{benzyltriethylammonium}$ ,  $\text{M} = \text{Mn}^{2+}, \text{Fe}^{2+}$ ). *New. J. Chem.* **27**, 779–782 (2003).
27. Thiele, G. & Messer, D. S-Thiocyanato- und N-Isothiocyanato-Bindungsisomerie in den Kristallstrukturen von  $\text{RbCd}(\text{SCN})_3$  und  $\text{CsCd}(\text{SCN})_3$ . *Z. Anorg. Allg. Chem.* **464**, 255–267 (1980).
28. Xie, K.-P. *et al.* Order-disorder phase transition in the first thiocyanate-bridged double perovskite-type coordination polymer:  $[\text{NH}_4]_2[\text{NiCd}(\text{SCN})_6]$ . *CrystEngComm* **18**, 4495–4498 (2016).
29. Hill, J. A., Thompson, A. L. & Goodwin, A. L. Dicyanometallates as model extended frameworks. *J. Am. Chem. Soc.* **138**, 5886–5896 (2016).
30. Lefebvre, J., Chartrand, D. & Leznoff, D. Synthesis, structure and magnetic properties of 2-D and 3-D  $[\text{cation}]\{\text{M}[\text{Au}(\text{CN})_2]_3\}$  ( $\text{M} = \text{Ni}, \text{Co}$ ) coordination polymers. *Polyhedron* **26**, 2189–2199 (2007).
31. Duyker, S. G., Hill, J. A., Howard, C. J. & Goodwin, A. L. Guest-activated forbidden tilts in a molecular perovskite analogue. *J. Am. Chem. Soc.* **138**, 11121–11123 (2016).

32. Boström, H. L. B., Hill, J. A. & Goodwin, A. L. Columnar shifts as symmetry-breaking degrees of freedom in molecular perovskites. *Phys. Chem. Chem. Phys.* **18**, 31881–31894 (2016).
33. Zhang, W., Cai, Y., Xiong, R.-G., Yoshikawa, H. & Awaga, K. Exceptional dielectric phase transitions in a perovskite-type cage compound. *Angew. Chem. Int. Ed.* **49**, 6608–6610 (2010).
34. Evans, N. L. *et al.* Control of multipolar and orbital order in perovskite-like  $[\text{C}(\text{NH}_2)_3]\text{Cu}_x\text{Cd}_{1-x}(\text{HCOO})_3$  metal–organic frameworks. *J. Am. Chem. Soc.* **138**, 9393–9396 (2016).
35. Goodwin, A. L. Rigid unit modes and intrinsic flexibility in linearly bridged framework structures. *Phys. Rev. B* **74**, 134302 (2006).
36. Hammonds, K. D., Dove, M. T., Giddy, A. P., Heine, V. & Winkler, B. Rigid-unit phonon modes and structural phase transitions in framework silicates. *Am. Mineral.* **81**, 1057–1079 (1996).
37. Dove, M. T., Heine, V. & Hammonds, K. D. Rigid unit modes in framework silicates. *Mineral Mag.* **59**, 629–639 (1995).
38. Weller, M. T., Weber, O. J., Henry, P. F., Di Pumpo, A. M. & Hansen, T. C. Complete structure and cation orientation in the perovskite photovoltaic methylammonium lead iodide between 100 and 352 K. *Chem. Commun.* **51**, 4180–4183 (2015).
39. Hatch, D. M. & Stokes, H. T. Invariants: Program for obtaining a list of invariant polynomials of the order parameter components associated with irreducible representations of a space group. *J. Appl. Cryst.* **36**, 951–952 (2003).
40. Lufaso, M. W. & Woodward, P. M. Prediction of the crystal structures of perovskites using the software program SPuDS. *Acta Cryst. B* **57**, 725–738 (2001).

41. Antsyshkina, A. S., Porai Koshits, M. A., Ostrikova, V. N. & Sadikov, G. G. Stereochemistry of double formates. Crystal structure of ammonium triformatocadmate,  $(\text{NH}_4)\text{Cd}(\text{CHO}_2)_3$  and  $\text{KCd}(\text{CHO}_2)_3$ . *Sov. J. Coord. Chem.* **9**, 855–858 (1983).
42. Gómez-Aguirre, L. C. *et al.* Room-temperature polar order in  $[\text{NH}_4][\text{Cd}(\text{HCOO})_3]$  — a hybrid inorganic–organic compound with a unique perovskite architecture. *Inorg. Chem.* **54**, 2109–2116 (2015).
43. Hu, K.-L., Kurmoo, M., Wang, Z. & Gao, S. Metal-organic perovskites: Synthesis, structures, and magnetic properties of  $[\text{C}(\text{NH}_2)_3][\text{M}^{\text{II}}(\text{HCOO})_3]$  ( $\text{M} = \text{Mn}, \text{Fe}, \text{Co}, \text{Ni}, \text{Cu},$  and  $\text{Zn}$ ;  $\text{C}(\text{NH}_2)_3 = \text{Guanidinium}$ ). *Chem. Eur. J.* **15**, 12050–12064 (2009).
44. Wang, Z. *et al.* Anionic NaCl-type frameworks of  $[\text{Mn}^{\text{II}}(\text{HCOO})_3]^-$ , templated by alkylammonium, exhibit weak ferromagnetism. *Dalton Trans.* 2209–2216 (2004).
45. Wang, X.-Y., Gan, L., Zhang, S.-W. & Gao, S. Perovskite-like metal formates with weak ferromagnetism and as precursors to amorphous materials. *Inorg. Chem.* **43**, 4615–4625 (2004).
46. Bovill, S. M. & Saines, P. J. Structure and magnetic properties of the  $\text{AB}(\text{HCO}_2)_3$  ( $\text{A} = \text{Rb}^+$  or  $\text{Cs}^+$ ,  $\text{B} = \text{Mn}^{2+}$ ,  $\text{Co}^{2+}$  or  $\text{Ni}^{2+}$ ) frameworks: probing the effect of size on the phase evolution of the ternary formates. *CrystEngComm* **17**, 8319–8326 (2015).
47. Collings, I. E. *et al.* Compositional dependence of anomalous thermal expansion in perovskite-like  $\text{ABX}_3$  formates. *Dalton Trans.* **45**, 4169–4178 (2016).
48. Stroppa, A. *et al.* Electric control of magnetization and interplay between orbital ordering and ferroelectricity in a multiferroic metal-organic framework. *Angew. Chem. Int. Ed.* **50**, 5847–5850 (2011).
49. Stroppa, A., Barone, P., Jain, P., Perez-Mato, J. M. & Picozzi, S. Hybrid improper ferroelectricity in a multiferroic and magnetoelectric metal-organic framework. *Adv. Mater.* **25**, 2284–2290 (2013).

50. Geng, F.-J. *et al.* Perovskite-type organic-inorganic hybrid nlo switches tuned by guest cations. *J. Mater. Chem. C* **5**, 1529–1536 (2017).
51. Campbell, B. J., Stokes, H. T., Tanner, D. E. & Hatch, D. M. ISODISPLACE: A web-based tool for exploring structural distortions. *J. Appl. Cryst.* **39**, 607–614 (2006).

**Acknowledgements** MSS acknowledges the Royal Commission for the Exhibition of 1851 and the Royal Society for fellowships.

**Author Contributions Statements** All authors designed the study and contributed to the writing of the paper. H.L.B.B. and M.S.S. performed the symmetry analysis.

**Competing Interests** The authors declare that they have no competing financial interests.

**Correspondence** Correspondence and requests for materials should be addressed to M.S.S. or A.L.G. (email: m.senn@warwick.ac.uk or andrew.goodwin@chem.ox.ac.uk).

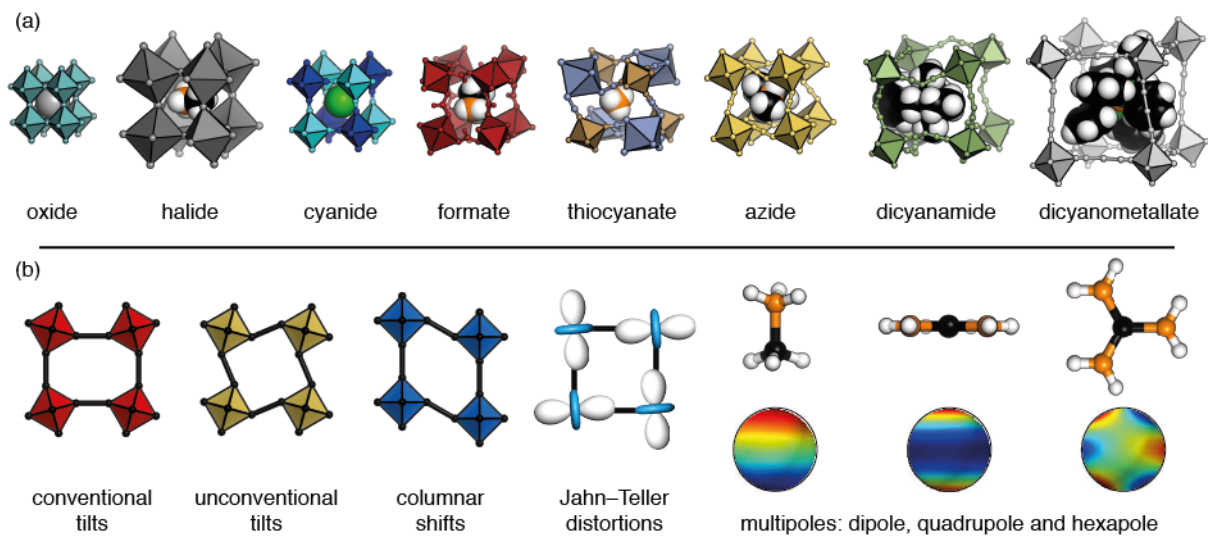


Figure 1: Molecular perovskites and their degrees of freedom. (a) A perovskite oxide with the molecular congeners shown to scale. In all cases, the A-site cation is shown as spacefilling, with carbon in black, hydrogen in white, nitrogen in orange and phosphorus in green. (b) schematic illustrations of the various degrees of freedom accessible to molecular perovskites.

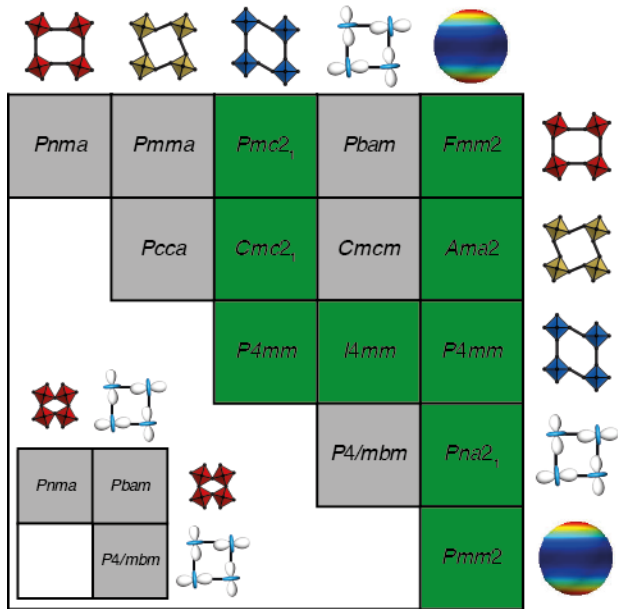


Figure 2: Coupling schemes of the accessible distortions: conventional tilts, unconventional tilting, columnar shifts, Jahn-Teller distortions, and multipole ordering. In each case, a representative space group is shown and the colour indicates whether the coupling can ever drive a polar distortion (green) or not (grey). The inset shows the corresponding coupling scheme for conventional inorganic perovskites.



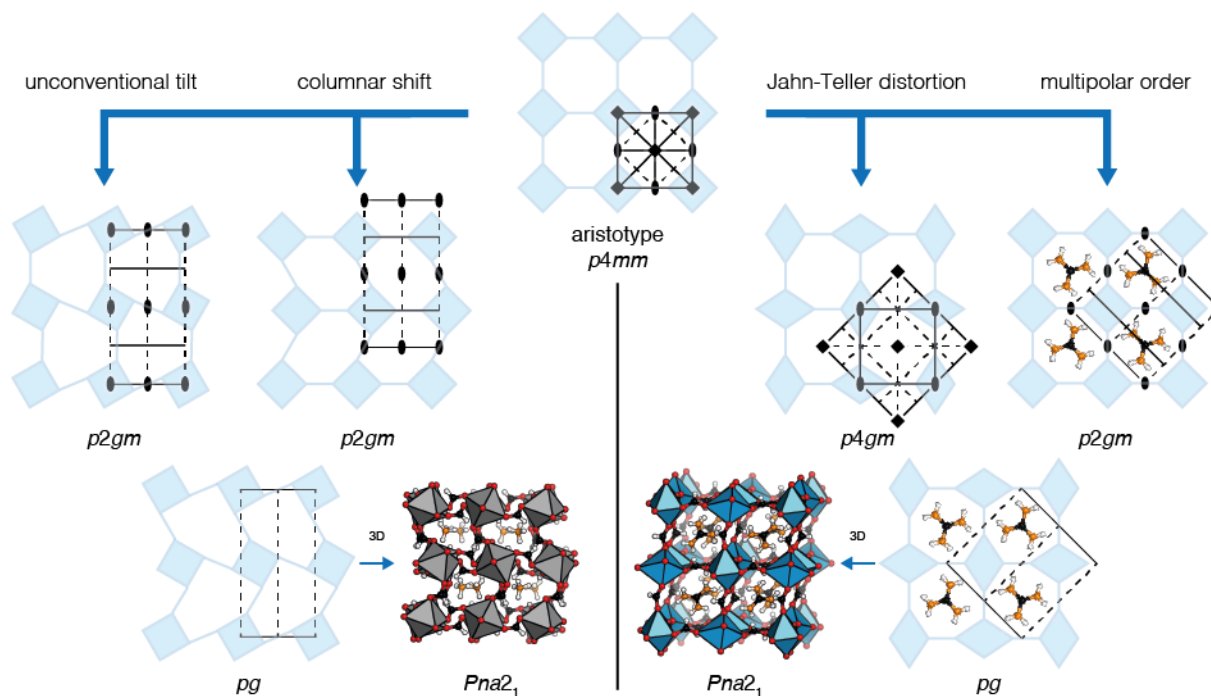


Figure 3: Inversion symmetry breaking in 2D molecular perovskites. Left: both unconventional tilting and columnar shifts yield the plane group  $p2gm$ , but with different origins. When coupled together, the resulting plane group is  $pg$ , which lacks inversion symmetry. A conceptually-related combination of octahedral tilts and shifts is responsible for inversion symmetry breaking in  $[\text{NH}_4]\text{Cd}(\text{HCOO})_3$ , which crystallises in  $Pna2_1$ . Right: a  $C$ -type cooperative Jahn–Teller distortion lowers 2D molecular perovskite symmetry to  $p4gm$ , whereas antiferrohexapolar order gives a  $p2gm$  cell with a different origin. When combined, the two distortions generate the polar plane group  $pg$ . This is a 2D analogue of the hybrid coupling found in  $\text{GuaCu}(\text{HCOO})_3$ .

Table 1: The irreps corresponding to the different distortions considered.

Distortion	Irreps
Conventional tilting	$\mathbf{M}_2^+, \mathbf{R}_5^-$
Unconventional tilting	$\Gamma_4^+, \mathbf{X}_{1,5}^-, \mathbf{M}_5^+$
Columnar shifts	$\Gamma_{3,4,5}^+, \mathbf{X}_5^+, \mathbf{M}_2^-$
Jahn-Teller distortions	$\mathbf{M}_3^+, \mathbf{R}_3^-$
Quadrupolar A-site order	$\Gamma_{3,5}^+, \mathbf{X}_{2,5}^+, \mathbf{M}_{1,2,4,5}^+, \mathbf{R}_5^+$
Dipolar A-site order	$\Gamma_4^-, \mathbf{X}_{3,5}^-, \mathbf{M}_{3,5}^-, \mathbf{R}_4^-$